

# Spectral Phase Retrieval by Dispersion-distorted Frequency-resolved Optical Gating Traces

Po-Ya Wu,\* and Shang-Da Yang

Institute of Photonics Technologies, National Tsing Hua University, Hsinchu 30013, Taiwan

\*Corresponding author: poyawu@ipt.nthu.edu.tw

## Abstract

A new algorithm is proposed to accurately reconstruct the spectral phase from frequency-resolved optical gating (FROG) traces seriously distorted by crystal dispersion and rippled phase-matching spectrum for the first time (to our best knowledge).

## I. INTRODUCTION

Self-referenced femtosecond pulse measurement techniques typically rely on crystal nonlinearity, such as second-harmonic generation (SHG), to achieve temporal gating or spectral shearing. Thin crystal is normally utilized to avoid (1) strong group velocity mismatch (GVM) walk-off [1], i.e. insufficient phase matching (PM) bandwidth, and (2) pulse distortion due to group velocity dispersion (GVD) [2]. GVM used to be dominant (except for few-cycle pulses), but has been overcome by using chirped quasi-phase matched (QPM) grating [3] or novel measurement technique [4,5]. As a result, GVD becomes the only limiting factor of the crystal thickness (thus conversion efficiency) in pulse measurement. For example, type-I BBO shorter than 40  $\mu\text{m}$  is needed to prevent 5-fs Ti/S laser pulses from broadening by 5%. In this contribution, we propose a modified algorithm to deal with frequency-resolved optical gating (FROG) traces [6] seriously distorted by GVD and rippled PM spectrum [3]. This is the first success (to our best knowledge) of eliminating the crystal thickness constraint imposed by GVD, which is promising in measuring weak few-cycle pulses.

## II. THEORY

The second-harmonic spectrum due to pulse replicas of individual spectrum  $E(\omega')$  and time delay  $\tau$  passing through a nonlinear crystal of length  $L$  is written as [7]

$$E_{2\omega}(\Omega, \tau) \propto \left( \frac{-j \cdot \Omega}{2 \cdot n_{2\omega}(\Omega) \cdot c_0} \right) \times e^{-jk_{2\omega}(\Omega)L} \times \left\{ \int_0^\infty E_\omega(\omega') e^{-j\omega'\tau} E_\omega(\Omega - \omega') \left[ \int_0^L d_{\text{eff}}(z) e^{j\Delta k} dz \right] d\omega' \right\}, \quad (1)$$

where  $d_{\text{eff}}(z)$  is the effective nonlinear coefficient, and  $\Delta k(\Omega, \omega') = k_{2\omega}(\Omega) - k_\omega(\omega') - k_\omega(\Omega - \omega')$  is the wave vector mismatch. When GVD is weak,  $\Delta k$  reduces to a function of  $\Omega$  and Eq. (1) is simplified to a transfer function relation

$$E_{2\omega}(\Omega, \tau) \propto \left( \frac{-j \cdot \Omega}{2 \cdot n_{2\omega}(\Omega) \cdot c_0} \right) F(\Omega) H(\Omega), \quad (2)$$

where  $F(\Omega) \propto \int_0^\infty E_\omega(\omega') e^{-j\omega'\tau} E_\omega(\Omega - \omega') d\omega'$  is the nonlinear polarization spectrum, and  $H(\Omega) = e^{-jk_{2\omega}(\Omega)L} \times \int_0^L d_{\text{eff}}(z) e^{j\Delta k} dz$  is the PM spectrum contributed by the crystal. Standard SHG FROG algorithms work well under the conditions of negligible GVD and flat  $H(\Omega)$ , which are violated if one uses a very long, chirped QPM grating [3]. We modify the traditional iterative algorithm in two aspects (Fig. 1). (1) The FROG trace is calculated by double integral [Eq. (1)], instead of the typical  $|F(\Omega)|^2$ . (2) The unknown spectral phase  $\Psi(\omega')$  is expanded by an  $N$ th-order polynomial around the fundamental central angular frequency  $\omega_0$

$$\Psi(\psi_2, \psi_3, \dots, \psi_N) = \sum_{n=2}^N \frac{\psi_n}{n!} (\omega' - \omega_0)^n. \quad (3)$$

The FROG error  $\varepsilon$  (a function of  $\psi_2, \dots, \psi_N$ ) between the actual and calculated FROG traces is minimized by the steepest descent method [8]. This means the set of  $\{\psi_n\}$  is repeatedly updated by moving in opposite direction of the (numerically calculated) gradient of  $\varepsilon$  by a proper distance in the  $(N-1)$ -dimensional space until  $\varepsilon$  is small enough. Note that the spectral phase representation can be replaced by expansion of other orthogonal basis functions (e.g. sinusoidal functions) or even arbitrary function of finite samplings.

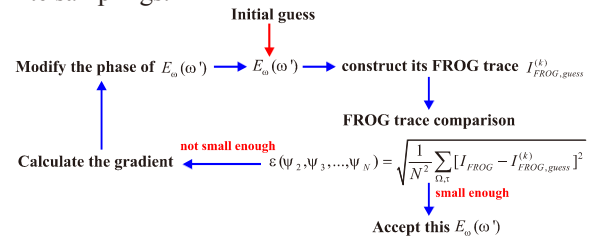


Fig. 1. Flow chart of the modified phase retrieval algorithm in this work.

## III. SIMULATION RESULTS

Consider a Gaussian spectrum [shaded, Fig. 2(c)] centered at 1550 nm and supporting a transform-limited pulse width (defined by FWHM) of 75 fs. FROG traces due to pulses with different spectral phases and a 6-cm-long aperiodically poled lithium niobate (A-PPLN) bulk [3] are calculated by Eq. (2). The linear poling period function  $\Lambda(z)$  between 20.28  $\mu\text{m}$  and 20.31  $\mu\text{m}$  of the A-PPLN bulk adequately preserves the second-harmonic bandwidth, while the 6-cm thickness can considerably distort the fundamental pulse. As a proof of concept, we

tested two different spectral phases approximated by third-order polynomials, i.e.  $N=3$  in Eq. (3).

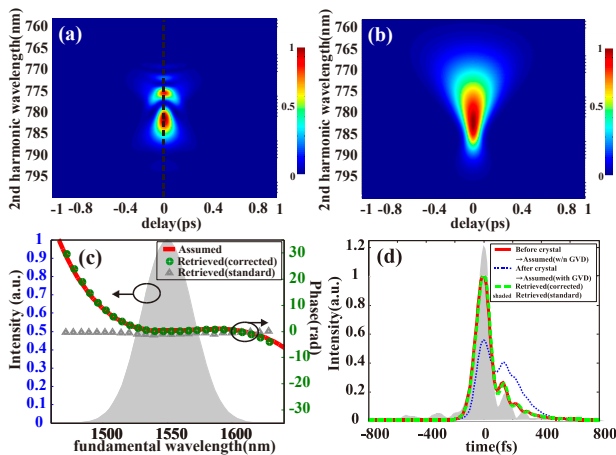


Fig. 2. (a) The original (left half) and retrieved (right half) FROG traces. (b) The ideal FROG trace due to extremely short crystal. (c) The power spectrum (shaded) and spectral phases retrieved by standard (triangles) and modified (circles) algorithms, respectively. (d) Temporal intensities of assumed pulse (red solid) and those retrieved by standard (shaded) and modified (green dashed) algorithms. The pulse after the 6-cm A-PPLN is shown for comparison (blue dotted).

Figure 2 shows the simulation results of Pulse 1 with a third-order polynomial phase curve represented by  $\psi_3=3.79 \times 10^{-4} \text{ ps}^3$ ,  $\psi_2=5.64 \times 10^{-3} \text{ ps}^2$  [solid, Fig. 2(c)]. The temporal intensity of the fundamental pulse [red solid, Fig. 2(d)] is stretched by more than two times and seriously distorted after passing through the 6-cm-long A-PPLN [blue dotted, Fig. 2(d)]. The corresponding FROG trace [left half, Fig. 2(a)] largely differs from the ideal one [Fig. 2(b)] in the presence of strong GVD and rippled PM spectrum. Spectral phase reconstruction from the distorted FROG trace (after frequency marginal correction to alleviate the ripple of PM spectrum) by the standard algorithm gives very poor result [triangles, Fig. 2(c)]. In contrast, our modified algorithm accurately retrieves the phase [circles, Fig. 2(c)] within 107 iterations. The temporal intensity from the given power spectrum and retrieved spectral phase [green dashed, Fig. 2(d)] agrees well with the assumed one [red solid, Fig. 2(d)], corresponding to a small root-mean-square (rms) error of  $1.58 \times 10^{-2}$  (calculated by normalizing the assumed curve to unit peak).

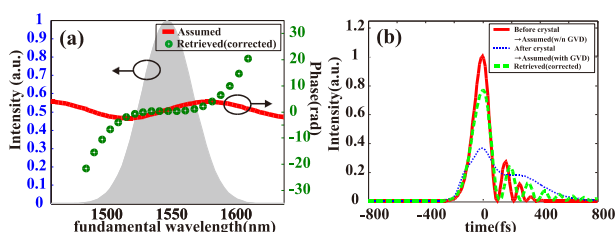


Fig. 3. (a) The spectral intensity and phase of the fundamental field. (b) Time domain pulse shape of the fundamental field.

Figure 3 shows the simulation results of Pulse 2 with a sinusoidal phase curve of amplitude  $\pi$  rad [solid, Fig. 3(a)]. The specific phase function is of practical

importance in ultrafast spectroscopy and can be used in testing the performance of polynomial expansion (considering typical tunable dispersion compensators can only handle the first few orders of spectral phases). The pulse shape is seriously distorted by the GVD [blue dotted, Fig. 3(b)], and one cannot expect reliable phase reconstruction by the standard FROG algorithm. The modified algorithm is hampered by local minimum in this case, giving an approximated third-order polynomial spectral phase [circles, Fig. 3(a)]. The corresponding temporal intensity [green dashed, Fig. 3(b)] resolves the main lobe and the first side lobe reasonably well, but exhibiting stronger oscillatory tail than the assumed one [red solid, Fig. 3(b)]. This is attributed to the fact that the sinusoidal phase cannot be well-approximated by a third-order polynomial.

#### IV. CONCLUSIONS

We have numerically demonstrated a modified FROG algorithm based on double integral-formulated SHG process and the steepest descent optimization, which can deal with FROG traces seriously distorted by GVD and rippled phase-matching spectrum. The spectral phase representation is currently limited to polynomials, but can readily be generalized to arbitrary curves at the cost of increased simulation complexity. This algorithm is promising in measuring low-power few-cycle pulses.

#### REFERENCES

- [1] A. M. Weiner, "Effect of group velocity mismatch on the measurement of ultrashort optical pulses via second harmonic generation", *IEEE J. Quantum Electron*, **19**, pp. 1276-1283, 1983.
- [2] X. Xiao, C. Yang, S. Gao, and H. Miao, "Analysis of ultrashort-pulse second-harmonic generation in both phase- and group-velocity-matched structures", *IEEE J. Quantum Electron*, **41**, pp. 85-93, 2005.
- [3] S. -D. Yang, A. M. Weiner, Krishnan R. Parameswaran, Martin M. Fejer "Ultrasensitive second-harmonic generation frequency-resolved optical gating by aperiodically poled LiNbO<sub>3</sub> waveguides at 1.5  $\mu\text{m}$ ", *Opt. Lett.*, **30**, 2164-2166, 2005.
- [4] S. -D. Yang, C. -S. Hsu, S. -L. Lin, Y. -S. Lin, C. Langrock, and M. M. Fejer, "Ultrasensitive direct-field retrieval of femtosecond pulses by modified interferometric field autocorrelation", *Opt. Lett.*, **34**, 3065-3067, 2009.
- [5] C. -S. Hsu, Y. -H. Lee, A. Yabushita, T. Kobayashi, and S. -D. Yang, "Spectral phase retrieval of 8 fs optical pulses at 600 nm by using a collinear autocorrelator with 300- $\mu\text{m}$ -thick lithium triborate crystals," *Opt. Lett.*, **36**, 11, 2041-2043, 2011.
- [6] R. Trebino, *Frequency-resolved Optical Gating: the measurement of ultrashort laser pulses*. Boston, MA, USA: Kluwer Academic Publishers, 2000.
- [7] A. M. Weiner, *Ultrafast Optics*, Chapter 5, John Wiley & Sons, Inc., 2009, pp. 198-257.
- [8] E. K. P. Chong, S. H. Zak, *An introduction to optimization*, 2nd edition, Wiley, 2001.